



# EPA Public Access

Author manuscript

*Environ Model Softw.* Author manuscript; available in PMC 2018 April 19.

About author manuscripts

Submit a manuscript

Published in final edited form as:

*Environ Model Softw.* 2017 ; 98: 21–34. doi:10.1016/j.envsoft.2017.09.004.

## A web-based screening tool for near-port air quality assessments

Vlad Isakov<sup>a,\*</sup>, Timothy M. Barzyk<sup>a</sup>, Elizabeth R. Smith<sup>a</sup>, Saravanan Arunachalam<sup>b</sup>, Brian Naess<sup>b</sup>, and Akula Venkatram<sup>c</sup>

<sup>a</sup>U.S. Environmental Protection Agency, Office of Research and Development, 109 Alexander Drive, Research Triangle Park, NC 27713, USA

<sup>b</sup>The University of North Carolina at Chapel Hill, Institute for the Environment, Chapel Hill, NC 27599, USA

<sup>c</sup>University of California Riverside, Bourns College of Engineering, Riverside, CA 92521, USA

### Abstract

The Community model for near-PORT applications (C-PORT) is a screening tool with an intended purpose of calculating differences in annual averaged concentration patterns and relative contributions of various source categories over the spatial domain within about 10 km of the port. C-PORT can inform decision-makers and concerned citizens about local air quality due to mobile source emissions related to commercial port activities. It allows users to visualize and evaluate different planning scenarios, helping them identify the best alternatives for making long-term decisions that protect community health and sustainability. The web-based, easy-to-use interface currently includes data from 21 seaports primarily in the Southeastern U.S., and has a map-based interface based on *Google Maps*. The tool was developed to visualize and assess changes in air quality due to changes in emissions and/or meteorology in order to analyze development scenarios, and is not intended to support or replace any regulatory models or programs.

### 1. Introduction

Ports are a critical feature of the U.S. economy. Seaport cargo activity supports the employment of more than 23 million people in the United States and contributes nearly \$4.6 trillion in total economic activity (AAPA, 2016). But for all the economic benefit they provide, the influx of ship, train, truck, and other activities of commercial ports can also negatively impact the local environment, putting residents of neighboring communities at higher risk to health impacts associated with increased air and water pollution (Rosenbaum et al., 2011). Because many of the nation's 360 commercial ports are located near disadvantaged and lower-income communities, ports also raise environmental justice issues. Community groups are becoming increasingly active in local initiatives that seek to mitigate potentially harmful environmental conditions. However, there is a lack of accessible tools that can be easily applied to study near-source pollution, and rapidly explore the benefits of

This is an open access article under the CC BY-NC-ND license (<http://creativecommons.org/licenses/by-nc-nd/4.0/>).

\*Corresponding author: V. Isakov Isakov.Vlad@epa.gov.

improvements to air quality or to weigh trade-offs associated with port expansion or modernization. To address this need, US EPA has developed several tools designed for communities to assess environmental hazards and find ways to mitigate exposures. These include a suite of web-based applications such as C-FERST (Zartarian et al., 2011), EJSCREEN (U.S. EPA, 2016) and C-LINE (Barzyk et al., 2015). To add to this suite of community tools, we are developing the Community model for near-PORT applications (C-PORT) to help assess air quality impacts from port terminals, ships, roadway traffic and other port-related sources potentially affecting the local community. The multiple modeling options within C-PORT are designed for a quick assessment and require limited technical expertise. The power of such a screening tool is to facilitate assessments through reduced computational time, and to evaluate and compare a suite of “what-if” scenarios. Thus, these web-based, easy-to-use tools can provide valuable insights for the community and can also assist with the decision-making process.

C-PORT currently has data for 21 sea-ports, mostly in the Southeastern U.S. The model represents multiple source types: Ships (while docked at terminal and underway), Rail, Road, On-terminal activity, and provides the opportunity to add/modify individual sources. C-PORT models multiple primary pollutants that are directly emitted: CO, SO<sub>2</sub>, NO<sub>x</sub>, PM<sub>2.5</sub> and select Mobile Source Air Toxics (benzene, formaldehyde, acetaldehyde, and acrolein). The model shows absolute concentrations as well as relative changes, and also displays monitor information from EPA’s Air Quality System (AQS). C-PORT model formulations are derived from dispersion theory, turbulence theory, and boundary layer meteorology. The algorithm for line sources is based on the analytical approximation for line sources (Venkatram and Horst, 2006), consistent with the US EPA research model for line sources R-LINE (Snyder et al., 2013). Algorithms for stationary and area sources are similar to AERMOD (Cimorelli et al., 2005), but optimized for computational efficiency to allow user interaction with the web-based modeling simulations in real-time. For example, C-PORT provides an initial parameterization of both meteorological (using National Weather Service data) and emissions data (based on spatially-allocated emissions values from EPA’s National Emissions Inventory) to facilitate the creation of dispersion scenarios.

We refer to C-PORT as a “screening” tool, designed to encourage its use by a non-expert stakeholder through computational efficiency coupled with a default set of emissions and meteorological inputs. The results obtained through its application are reliable enough to screen for situations that might require further analysis to examine the impact of the source under a range of inputs not included in the default set. The term “screening” should not be confused with the formal term “screening model” defined in the Guideline on Air Quality Models (<https://www.federalregister.gov/documents/2017/01/17/2016-31747/revisions-to-the-guideline-on-air-quality-models-enhancements-to-the-aermod-dispersion-modeling>) as a model that provides conservative (maximum) estimates of the air quality impact of a specific source. C-PORT is not intended for regulatory applications, enforcement, or refined analysis intended to meet EPA Guideline on Air Quality Models Appendix W requirements (40 CFR Appendix W to part 51).

This paper describes the model structure, input parameters, dispersion algorithms and evaluation, mapping and visualization routines, and software considerations for C-PORT. We

also discuss the model functionality using an example application for an area in the port of Charleston, SC.

## 2. Methods

### 2.1. Model design

The modeling system includes dispersion algorithms for area, point, and line sources related to freight-movement activities, and emissions from the port terminals. C-PORT automatically accesses pre-loaded emissions and meteorological datasets with nationwide coverage and provides results for the user-defined geographic area as both visualized maps and tabular data. The key model inputs include emissions and meteorology, and model outputs are presented as geospatial maps with some options to save the results as GIS shape files for further analysis.

C-PORT also allows the user to add, delete, and modify emissions sources. For example, in a hypothetical scenario where the port wants to expand a terminal (e.g. a bulk cargo terminal), C-PORT can simulate the effect of additional berth and cargo handling facilities in the port terminal. The user can manually draw a polygon to represent a new terminal using the web-interface, and double click on the last vertex to finish the polygon. For convenience, C-PORT assigns pre-populated emissions values for the new source. These values are computed as an average of the 10 nearest area sources. If additional emissions information for the new source is available, the user can edit the default values to reflect the new values. Similar to the area source representing a new terminal, the user can add a new point source to represent the hoteling location, or new roadway or rail line.

Analysis capabilities are provided through an easy-to-use GUI that can be used by community planners, port authority, and federal and state/local agency analysts, to assess air quality impacts of ‘what if’ scenarios for planning a sustainable development at community scales. These scenarios can help to anticipate potential growth in port activities (increased ships, trucks, etc.), assess impacts of improved energy efficiency and other voluntary actions in port terminal area activities (such as electrification of cranes or rubber tire gentries), and quantify reductions in emissions due to regulatory programs related to commercial marine vessels, rail, trucks, etc.

**2.1.1. Dispersion model algorithms**—This section describes dispersion algorithms used in C-PORT to produce the near-source air pollutant concentration gradients. C-PORT has several options for simulating dispersion of primary pollutants from emission sources in the port areas: on-terminal activity including drayage and cargo handling equipment (modeled as area sources); facilities with known latitude/longitude location within the port’s terminal (modeled as point sources); roads and rail (modeled as line sources); and finally ships-in-transit (modeled as line sources with plume rise). The dispersion algorithms in C-PORT are similar to the dispersion tools used by regulators and research scientists, but have been modified slightly to speed computational time and enable quick access to results. The dispersion code for area and point sources is based upon model formulations used in AERMOD (Cimorelli et al., 2005), while the road and rail are modeled as line sources,

based upon an analytical approximation (Venkatram and Horst, 2006) that is used in the C-LINE modeling system (Barzyk et al., 2015).

The C-PORT modeling system achieves its computational efficiency by 1) using analytical forms when possible to replace the numerical schemes in AERMOD, 2) using less-stringent iteration schemes for convergence than those in AERMOD, and 3) avoiding computationally demanding, iterative algorithms. These differences include limiting the number of line sources in the area source algorithm to 30 for computational efficiency as opposed to the iterative process in AERMOD. For point sources, dispersion in the Convective Boundary Layer (CBL) is modeled using the Gaussian dispersion equation in which the plume spreads are formulated in terms of turbulence parameters computed at effective plume height. Also, C-PORT applies a simple algorithm that does not re-entrain plume material to determine the fraction of the emissions that can potentially affect ground-level concentrations. In the Stable Boundary Layer (SBL), vertical plume spread during stable conditions is limited by the height of the boundary layer. Unlike AERMOD, C-PORT does not treat dispersion in complex terrain and does not account for building effects like downwash.

Normalized concentration estimates from C-PORT were compared with estimates from AERMOD and R-LINE for several scenarios of hypothetical source configurations over a range of meteorological conditions. The sources consisted of 1) a point source representing a stationary source at port terminals, 2) an area source representing a port terminal, and 3) a line source, representing a portion of a highway. For the point source test, we ran C-PORT and AERMOD for several configurations as a function of stack height: 10 m, 20 m, 30 m; stack diameter: 0.5 m; stack temperature: 100 and 200°C; and, exit velocity: 5 and 10 m/s. Receptors were placed 100 m apart up to 5000 m downwind from the source to capture the impact of the plume. For the area source test, we ran C-PORT and AERMOD for a single configuration, a 500 m × 400 m rectangular area source with downwind receptors at 10 m resolution within the first 100 m from the source, then at 50 m resolution in the 100–350 m zone, and at 100 m resolution beyond 300 m up to 3 km. For the line source test, we ran C-PORT and R-LINE for a single configuration, 1-km long line source and, with downwind receptors at 10 m resolution within 100 m from the source, 50 m resolution in the 100–350 m zone, and at 100 m resolution in the 300–3000 m zone. The sensitivity runs were conducted for a range of various meteorological conditions, stable, neutral, and convective stability conditions in summer and winter, and wind directions varying from 0 to 80°. Meteorological parameters are shown in the Appendix, Table S1.

For the area and point source tests, the model comparison measures are described in terms of the deviation of C-PORT estimates from those of AERMOD using the normalized residual,  $\varepsilon = (C_{\text{C-PORT}} - C_{\text{AERMOD}}) / \text{mean}(C_{\text{AERMOD}})$ , where  $C_{\text{C-PORT}}$  and  $C_{\text{AERMOD}}$  refer to concentration estimates from these two models. For the line source test, the comparison was between C-PORT and R-LINE. The residuals are computed using concentration estimates at receptors within the first 1000 m from the source for the line and area source tests and within the 5000 m from the source for the point source test. Zero values were excluded. The mean of  $\varepsilon$  measures the bias of the model relative to AERMOD for the area and point source tests and R-LINE for the line source test, and the standard deviation measures the scatter of

the bias. We used normalized bias  $NB(\overline{C_1 - C_2})/(\overline{C_2})$  and standard error  $SE = std(C_1 - C_2) / \sqrt{N}$  as quantitative model comparison measures. Normalized bias is a measure of the systematic bias of the model and is ideally equal to zero. Standard error measures the relative scatter and is smaller for better model performance (=0, ideally). These metrics are typically used to evaluate the model performance against observational data, but here we use them to quantify differences between two models ( $\overline{C_1}$  refers to concentrations from C-PORT and  $\overline{C_2}$  refers to concentrations from AERMOD for area and point source tests and R-LINE for the line source test). The plots comparing C-PORT estimates to corresponding estimates from AERMOD and R-LINE and tables of quantitative model comparison measures are shown in the Appendix (Figs. S1–S13). For these simplified scenarios of hypothetical source configurations (e.g., flat terrain, no building effects), the comparison indicates that the differences between C-PORT model algorithms and AERMOD are on average within 15% or better for area sources and within a factor of 2 for point sources. For line sources, the C-PORT predictions are within 5% of the corresponding R-LINE results.

**2.1.1.1. Dispersion algorithm for point sources:** The dispersion algorithm for point sources is designed to model point sources representing emissions from stacks or ships docked at the port terminals (Fig. 1). As in AERMOD, the model assumes that the concentration distributions in the vertical and horizontal are Gaussian except for convective conditions, where AERMOD uses a bi-Gaussian distribution.

The plume rise is calculated using the following equations. The plume rise  $h_p$  is taken to be (Weil, 1988)

$$h_p = \left[ \left( \frac{r_s}{\beta} \right)^3 + \frac{3}{U\beta^2} \left( F_m t + \frac{F_b}{2} t^2 \right) \right]^{1/3} - \frac{r_s}{\beta} \quad (1)$$

where  $\beta = 0.6$  is an entrainment coefficient,  $r_s$  is the stack exit radius,  $U$  is the average wind speed that governs plume rise, and  $t = x/U$  is the travel time to the downwind distance,  $x$ . In the equation,  $F_m$  and  $F_b$  are the momentum and buoyancy parameters given by

$$F_m = r_s^2 v_s^2 \quad (2)$$

$$F_b = \frac{g}{T_s} v_s r_s^2 (T_s - T_a)$$

where the subscript 's' refers to stack parameters, 'a' refers to ambient conditions,  $v_s$  is the stack exit velocity and  $T_s$  is stack exit temperature. In most cases, the momentum flux can be neglected in comparison to the buoyancy flux.

The plume rise is limited either by the temperature gradient in a stable boundary layer or the turbulence in a convective boundary layer. In a stable boundary layer, the maximum plume rise is given by

$$h_p(\text{max}) = \left( \frac{6 F_b}{\beta^2 U N^2} \right)^{1/3}, \quad (3)$$

where  $N$  is the Brunt-Vaisala frequency  $N = \left( \frac{g}{T} \frac{d\theta}{dz} \right)^{1/2}$  at plume height.

Under unstable conditions, we assume that the plume rise achieves its maximum rise when  $\frac{dh}{dt} = \sigma_w$ , which yields

$$h_p(\text{max}) = \left( \frac{2}{3\beta^2} \right) \frac{F_b}{U\sigma_w^2} \quad (4)$$

The meteorological parameters (i.e. Brunt-Vaisala frequency  $N$ , wind speed  $U$ , and vertical velocity fluctuation  $\sigma_w$ ), are evaluated at  $h_e = h_s + h_p/2$  by using boundary layer profiles. Because the plume rise is not known, the meteorological parameters at stack height are first used to calculate plume rise. Then, plume rise is calculated again using the meteorological parameters corresponding to the first estimate of plume rise.

As in AERMOD, the vertical plume spread is calculated by interpolating between surface formulations, and those corresponding to elevated releases. The vertical spread of the plume  $\sigma_z$  for a surface release is described by equations used in AERMOD (Cimorelli et al., 2005), which is representative of the current generation of dispersion models:

$$\begin{aligned} \sigma_z &= \sqrt{\frac{2}{\pi}} \frac{u_* x}{U} \left( 1 + 0.7 \frac{x}{L} \right)^{-1/3} \quad L > 0.0 \quad (5) \\ &= \sqrt{\frac{2}{\pi}} \frac{u_* x}{U} \left( 1 + 0.006 \left( \frac{x}{|L|} \right)^2 \right)^{-1/2} \quad L < 0.0 \end{aligned}$$

where  $L$  is the Monin-Obukhov length defined by  $L = -T_0 u_*^3 / (\kappa g Q_0)$ , where  $Q_0$  is the surface kinematic heat flux,  $u_*$  is the surface friction velocity,  $g$  is the acceleration due to gravity,  $T_0$  is a reference temperature, and  $\kappa$  is the Von Karman constant taken to be 0.40.

The horizontal spread of the plume is based on the equations in AERMOD (Cimorelli et al., 2005):

$$\sigma_y = \frac{\sigma_v x}{U} (1 + 78X)^{-0.3} \quad (6)$$

where

$$X = \frac{\sigma_v x}{U z_i}$$

and  $z_i$  is the mixed layer height.

The vertical spread of an elevated release is taken to be

$$\sigma_z = \frac{\sigma_w t}{(1 + t/2T_{Lw})^{1/2}} \quad (7)$$

Under stable conditions, the Lagrangian time scale,  $T_{Lw}$ , is taken to be (Venkatram et al., 1984)

$$T_{Lw} = \frac{l}{\sigma_w} \quad (8)$$

$$\frac{1}{l} = \frac{1}{l_s} + \frac{1}{l_n}$$

$$l_s = 0.27 \frac{\sigma_w}{N}; \quad l_n = 0.36 h_e$$

Under unstable conditions, the expression is

$$T_{Lw} = \frac{l}{\sigma_w} \quad (9)$$

$$l = 0.36 h_e$$

In Equations (8) and (9),  $h_e$  is the effective plume height. The expressions for  $\sigma_z$  corresponding to surface and elevated releases are combined using a weighting factor that accounts for the effective plume height relative to the boundary layer height,

$$\sigma_z = (1 - f)\sigma_{z(surface)} + f\sigma_{z(elevated)} \quad (10)$$

$$f = \min(1, h_{eff}/0.1z_i)$$

so that a source with an effective height of greater than 0.1  $z_i$  is taken to be an elevated source.

When the plume penetrates the capping inversion at the top of the mixed layer,  $z_i$  only part of the plume material contributes to ground-level concentrations. We account for this effect using a simple formulation similar to one included in the Danish “*Operationelle Meteorologiske Luftkvalitetsmodeller*” (OML) model (Olesen et al., 2007), where the emission rate,  $Q$ , is multiplied by a plume penetration factor,  $p_f$

$$p_f = \min(\max((z_i - h_s)/h_p, 0), 1) \quad (11)$$

and when the plume penetrates the capping inversion, the effective stack height is taken to be  $z_i$

$$h_e = p_f h_p + h_s \quad (12)$$

**2.1.1.2. Dispersion algorithm for line sources:** The dispersion algorithm for line sources is designed to efficiently model line sources representing emissions from roadway traffic and rail (Fig. 2). The dispersion algorithm that calculates near-road pollution profiles is described in more detail in Barzyk et al. (2015). Here we present the main features of the algorithm.

We represent a highway as a set of line sources located at the center of each lane of the highway. Each line source is represented as a set of elemental point sources. The contribution of the elemental point source,  $dC$ , located at  $(0, Y_s)$  to the concentration at  $(X_r, Y_r, Z_r)$  is taken to be given by the Gaussian plume formulation,

$$dC = \frac{qdY_s}{2\pi U \sigma_y(X_r) \sigma_z(X_r)} \exp\left(-\frac{Y_r^2}{2\sigma_y^2(X_r)}\right) F(Z_r) \quad (13)$$

where  $F(Z_r)$  is the vertical distribution function given by

$$F(Z_r) = \exp\left(-\frac{(z_s - Z_r)^2}{2\sigma_z^2}\right) + \exp\left(-\frac{(z_s + Z_r)^2}{2\sigma_z^2}\right) \quad (14)$$

where  $\sigma_y$  and  $\sigma_z$  are the horizontal and vertical plume spreads. The second term on the right hand side of Equation (14) accounts for plume reflection from the ground.

The contribution of a line source to the concentrations at a receptor  $(X_r, Y_r)$  is given by the integral of the contributions of the point sources along the line,



$$C(X_r, Y_r) = \int_{Y_1}^{Y_1+L} dC \quad (15)$$

This integral can be integrated numerically but the computational cost becomes unmanageable if we have to estimate the impact of the large number of roads typical of an urban area. So the model is based on an analytical approximation to the integral, given by Venkatram and Horst (2006),

$$C_p(X_r, Y_r) \approx \frac{qF(Z_r)}{\sqrt{2\pi}U\sigma_z(X_r^{eff})\cos\theta} [\text{erf}(t_1) - \text{erf}(t_2)] \quad (16)$$

where

$$X_r^{eff} = X_r/\cos\theta \quad (17)$$

$$t_i = \frac{(Y_r - Y_i)\cos\theta - X_r\sin\theta}{\sqrt{2}\sigma_y(X_i)} \quad (18)$$

where  $q$  is the emission rate per unit length of the line source and  $\theta$  is the angle between wind direction and normal to the road. Here  $\sigma_y$  is evaluated at  $X_i \equiv X_r$  ( $Y_s = Y_j$ ). The definitions of  $t_1$  and  $t_2$  correspond to downwind distances,  $X_r$ , from the end points  $Y_1$  and  $Y_2$  of the line to the receptor at  $(X_r, Y_r)$ . We see from Fig. 3 that the vertical spread in Equation (16) is evaluated at a downwind distance from the line source along the wind direction. The vertical and horizontal plume spreads are computed using formulations, described earlier, for point sources.

Equation (16) breaks down at  $\theta = 90^\circ$  because of the term  $\cos\theta$  in the denominator. We can avoid the problem at  $\theta = 90^\circ$  by noticing that for linear vertical spread the product

$$\sigma_z \left( \frac{X_r}{\cos\theta} \right) \cos\theta = \sigma_z(X_r)$$

in the denominator of Equation (16). It turns out that this limit is

consistent with the exact solution of the integral for a parallel wind when the vertical and horizontal plume spreads are linear. So we account for this limit by setting the denominator in the equation to  $(\sigma_z(X_r) + \sigma_z(X_r/\cos\theta)\cos\theta)/2$ . Comparison with the numerical solution indicates that this approach leads to an error of less than 25% when  $\theta$  approaches  $90^\circ$ .

Under low wind speeds, horizontal meandering of the wind spreads the plume over large azimuth angles, which might lead to concentrations upwind relative to the vector averaged wind direction. AERMOD (Cimorelli et al., 2005), and other currently used regulatory

models (e.g. ADMS (Atmospheric Dispersion Modeling System), Carruthers et al., 1994), attempt to treat this situation by assuming that when the mean wind speed is close to zero, the horizontal plume spread covers  $360^\circ$ . In the random spread state, the release is allowed to spread radially in all horizontal directions. The concentration from a point source with an emission rate,  $Q$  is then given by:

$$C(x, y) = \sqrt{\frac{2}{\pi}} \frac{Q}{2\pi r U_e \sigma_z(r)} \quad (19)$$

where  $r$  the distance between the source and receptor and the plume spread covers  $2\pi$  radians. The plume is transported at an effective velocity given by

$$U_e = (\sigma_u^2 + \sigma_v^2 + U^2)^{1/2} = (2\sigma_v^2 + U^2)^{1/2} \quad (20)$$

where  $U$  is the mean vector velocity, and the expression assumes that  $\sigma_v \approx \sigma_u$ . Note that the effective velocity is non-zero even when the mean velocity is zero. The minimum value of the transport wind,  $U_e$ , is  $\sqrt{2}\sigma_v$ .

If we assume that the vertical plume spread is linear with distance, the integral of the contributions of the meandering components of the point sources along the line source can be written as

$$C_m(X_r, Y_r) = \sqrt{\frac{2}{\pi}} \frac{qF(Z_r) \theta_s}{U \sigma_z(X_r) 2\pi} \quad (21)$$

where  $\theta_s$  is the angle subtended by the line source at the receptor,

$$\theta_s = \tan^{-1}\left(\frac{Y_2 - Y_1}{X_r}\right) + \tan^{-1}\left(\frac{Y_r - Y_1}{X_r}\right) \quad (22)$$

We assume that Equation (21) is a useful approximation even when vertical plume spread is not linear. Note that  $\theta_s$  is the angle subtended by the line source at the receptor. So the maximum value of this subtended angle is  $\pi$  when the receptor is very close to the line.

The success of this meandering adjustment in AERMOD depends on measurements of  $\sigma_v$ , which reflect meandering when the wind speed is close to zero. If measurements are not available  $\sigma_v$  is estimated from the approximation (Cirillo and Polli, 1992)

$$\sigma_v^2 = u^2 \sinh(\sigma_\theta^2) \quad (23)$$

where  $\sigma_\theta$  is the measured standard deviation of the horizontal velocity fluctuations.

Then, the concentration at a receptor is taken to be a weighted average of concentrations of two possible states: a random spread state, Equation (21), and a plume state, Equation (16).

$$C = C_p(1 - f_r) + C_m f_r \quad (24)$$

The weight for the random component in Equation (24) is taken to be

$$f_r = \frac{2\sigma_v^2}{U_e^2} \quad (25)$$

This ensures that the weight for the random component goes to unity when the mean wind approaches zero.

The need to specify an effective wind speed,  $U$ , used in the dispersion model highlights a problem with the application of the Gaussian dispersion equation to releases in the surface layer, where the wind speed varies with height. However, if the source height and the receptor height are close to zero, and the receptor is close to the line source, the ground-level concentration is insensitive to the choice of the height to evaluate the wind speed because the ground-level concentration is inversely proportional to the product  $\sigma_z U$ , which is independent of  $U$ . At this point, there is no consensus on the evaluation of the effective wind speed. The wind speed,  $U$ , is computed at the mean plume height,  $\bar{z}$ , by solving the following equation iteratively,

$$\sigma_z = f(x, u^*, L, U(\bar{z})) \quad (26)$$

where the mean plume height for a Gaussian distribution is given by

$$\bar{z} = \sigma_z \sqrt{\frac{2}{\pi}} \exp\left[-\frac{1}{2}\left(\frac{z_s}{\sigma_z}\right)^2\right] + z_s \operatorname{erf}\left(\frac{z_s}{\sqrt{2}\sigma_z}\right) \quad (27)$$

where the right hand side of Equation (26) corresponds to the expressions for vertical spread given by Equation (5).

**2.1.1.3. Dispersion algorithm for buoyant line sources:** One of the novel features of the C-PORT modeling system is the dispersion algorithm that calculates near-source pollution gradients for buoyant line sources. The dispersion algorithm is designed to specifically model moving line sources such as ships in transit (Fig. 3).

A moving ship is essentially a point source that moves along a line. Assuming that the averaging time for the calculation is long compared to the transit time of the ship, we can

model the moving ship as a line source laid along its path. This source has buoyancy corresponding to the exhaust gases of the ship. We describe the line source using the earlier equations, where the effective release height is the stack height plus plume rise, computed using an algorithm for a point source. C-PORT assigns the following stack parameters as a default option: stack height  $h=20$  m, stack diameter  $d=0.8$  m, temperature  $T=282\text{C}$ , exit velocity  $v=4$  m/s. C-PORT also allows the user to change the default stack parameters for each segment of the shipping channel.

**2.1.1.4. Dispersion algorithm for area sources:** The dispersion algorithm is designed to efficiently model area sources representing emission sources such as dray trucks or rubber tire gentry at port terminals (Fig. 4). As in AERMOD, an area source is treated as a polygon as shown in Fig. 4. The emissions from the area source are distributed among a set of line sources that are perpendicular to the near surface wind.

Because the wind is perpendicular to each line source, the expression for the contribution for each line source becomes:

$$C_p(X_r, Y_r) = \frac{qF(Z_r)}{\sqrt{2\pi}U\sigma_z(X_r - X_s)} [\text{erf}(t_1) - \text{erf}(t_2)] \quad (28)$$

where

$$t_i = \frac{(Y_r - Y_{si})}{\sqrt{2}\sigma_y(X_r - X_s)} \quad (29)$$

and  $X_r$  and  $Y_r$  are the co-ordinates of the receptor in the co-ordinate system with the x-axis along the mean wind. Here  $X_s$  is the coordinate of the line source with end points,  $Y_{si}$  determined by the intersection of the line with the sides of the polygon. In AERMOD, the number of line sources is increased until the successive values of the sums of their contributions is smaller than a specified value: the integral representing the area source converges within a specified error. In the C-PORT version of the algorithm, we reduce the computational demands of the area source algorithm by restricting the number of line sources to 30.

**2.1.2. Model inputs – emissions—**C-PORT includes emissions inventories based on EPA National Emissions Inventories (NEI)-2011 (<https://www.epa.gov/air-emissions-inventories/2011-national-emissions-inventory-nei-data>) from the following key source categories: 1) port terminals, 2) ships, 3) roadways, 4) rail. Users can run the model with the included data or input their own locally-derived values. Then, emissions are spatially allocated at the local level.

The first category, port terminals, includes emissions from drayage and cargo handling equipment, and all other “on-terminal” activities. Non-mobile sources include facilities with latitude/longitude coordinates located within terminal boundaries (port terminal boundaries

were identified using ArcGIS). Any facilities with latitude/longitude location (and not rail), and that falls within the port's terminal boundary is modeled as an explicit point source. The drayage and cargo handling equipment, and all other "on-terminal" activities emissions are allocated to terminals and modeled as area sources.

The ship emissions include ocean going vessels (Class III) and harbor craft emissions from Class I and II vessels. Harbor craft emissions are allocated to terminals and modeled as area sources. Class I, II emissions are also allocated to the channels. Emissions from ocean going vessels hoteling at the terminal are allocated to terminals and modeled as point sources, and emissions from ships underway are allocated to shipping channels representing a path to the terminal from the sea (based on US Army Corps of Engineers shipping lane segments with freight activity), and modeled as line sources with plume rise.

The rail category includes emissions from railroad equipment, line haul locomotives and yard locomotives. Railroad emissions are allocated to railroads using ArcGIS and modeled as line sources, and rail yard emissions are allocated to rail yard polygons in ArcGIS modeled as area sources. Users can assign their own emissions inputs for these locations or use the default estimates provided, based upon NEI 2011.

Roadway emissions are based on a combination of road network, traffic activity and emissions factors. The first input variable to consider is the road network for a given area. A road network is the system of interconnected roadways, and a description of their types (e.g., principal arterials such as interstates). In C-PORT version 3.0, the source for the road network is HPMS 2013 (<https://www.fhwa.dot.gov/policyinformation/hpms/fieldmanual/>). The HPMS road network consists of the National Highway System (NHS) routes (including intermodal connectors) and all other roads, excluding those functionally classified as minor collectors in rural areas and local roads. Traffic activity describes the number, types, and speeds of vehicles on a given roadway and for a given time period. Emissions factors are emission rates normalized by an activity basis, such as mass of pollutant per unit time or per mile, and based on vehicle type. The on-road data (activities, emission factor tables, monthly and county cross reference) were used from NEI2011v1, which were based on MOtor Vehicle Emission Simulator (MOVES) 2010b (U.S. EPA, 2012) in C-PORT version 3.0. The updated emissions, based on MOVES2014a emission factors and road types are used in C-PORT beta version 4.0. The activity data include annual average daily traffic (AADT) per road segment from the HPMS 2013 database. Most road segments have AADT values. For those segments that don't have corresponding AADT values, county-wide (or statewide in some cases) AADT averages by road type are used. Speeds for road segments come from NEI2011 v2 values. These are assigned to road segments by county average speeds by road class. For those road type combinations that don't have corresponding values in NEI, the national average values are used for the closest road type match. The emission factor (EF) tables include factors for three modes: rate per distance, rate per vehicle, and rate per profile, and we chose the EFs for rate per distance. The EFs were available for two separate months: January representing winter months such as Jan, Feb, Mar, Apr, Oct, Nov, and Dec; and July representing summer months such as May, Jun, Jul, Aug, and Sep. The roadways emissions in C-PORT are consistent with C-LINE web-based model (Barzyk et al., 2015) that estimates air quality impacts of traffic emissions for roadways in the U.S. (<https://>

[www.epa.gov/healthresearch/community-line-source-model-c-line-estimate-roadway-emissions](http://www.epa.gov/healthresearch/community-line-source-model-c-line-estimate-roadway-emissions)). Specific emissions for each road link are calculated by combining national database information on traffic volume and fleet mix with emissions factors from EPA's MOVES modeling system, as described in more detail in Barzyk et al. (2015).

**2.1.3. Model inputs – meteorology**—Meteorological inputs include hourly observations of wind speed and direction, ambient temperature, and other atmospheric boundary layer parameters needed for dispersion modeling. For calculating the representative hours, C-PORT uses hourly weather measurements from the National Weather Service (NWS) monitoring site that is nearest to the study location for 2011 and allows the user to simulate hourly concentrations for any of five representative meteorological conditions: 1) Stable, 2) Slightly Stable, 3) Neutral, 4) Slightly Convective, and 5) Convective), and for each season (Winter & Summer). These data were processed through AERMET, a meteorological data preprocessor for AERMOD ([https://www3.epa.gov/scram001/metobsdata\\_procaccprogs.htm](https://www3.epa.gov/scram001/metobsdata_procaccprogs.htm)). November-March and May-September periods are categorized as winter and summer seasons, respectively. To find the representative meteorological conditions, the valid measured hours are separated into Stable (Monin-Obukov Length ( $L$ ) > 0) and Convective ( $L$  < 0) conditions. These subsets are then ranked by  $L$ -value, from smallest to largest. The “Stable” hour is selected as the 5th-percentile ranked hour, then “Slightly Stable” hour is selected as the 50th-percentile ranked hour. Likewise, when the convective hours are ranked from smallest to largest ( $L$  is negative in Convective conditions), the “Convective” hour is selected as the 95th-percentile ranked hour, and the “Slightly Convective” hour is selected as the 50th-percentile ranked hour. The “Neutral” hour is selected when all hours are ranked by the absolute value of their  $L$ -value and the 99th-percentile ranked hour is selected. In all cases, the selected hour contains the wind speed,  $u_{Star}$ ,  $w_{Star}$ , convective mixing height, mechanical mixing height,  $L$ , surface roughness, and reference height.

The same 2011 NWS measurements are used to estimate annual averages. The annual averaging procedure is based on 100 representative meteorological hours for each station. These 100 h include a combination of 5 wind speeds, 4 wind directions and 5 stability conditions. The dispersion algorithm is run explicitly for the 100 h, and then weighted by frequency (how often these 100 h occur in the annual dataset) to estimate the annual averages. This method called the METeorologically-weighted Averaging for Risk and Exposure (METARE) is described further in Chang et al. (2015). Chang et al. (2015) compared model results using the METARE method (100 h) versus the explicit annual average method (based on full set of 8760 h) and found less than 10% difference over all receptors in a large urban area.

**2.1.4. Model receptors and maps**—C-PORT calculates air pollutant concentrations at a set of points in the modeling domain; these points are termed, “model receptors.” A regularly-spaced grid of receptors is generated for all source types. The grid consists of 50 by 50 evenly spaced grid points, which span the entire user's view window depending on zoom level. For line sources (roads, railways, and ships in transit), a series of receptors are placed perpendicular to each line source. Each perpendicular series consists of 5 receptors:

one on the source, two at 5 m off the source in each direction, and two at 25 m off the source. These perpendicular transects are created along the length of the line source. The spacing along the length of the source (for these transects; again, depending on the zoom level) can be 200 m, 500 m, or 1000 m. For shorter line segments, transects are placed at the midpoint of the segment. To reduce run complexity, annual average runs only use the uniform grid of receptors, not source-specific receptors. Hourly concentrations are calculated at all receptor locations. These calculated concentrations are used to generate the maps that C-PORT presents to users. We use a bi-linear interpolation algorithm from Scientific python (<http://docs.scipy.org/doc/scipy-0.15.1/reference/generated/scipy.interpolate.griddata.html>) to produce a gradient map of estimated pollutant concentrations. The color scheme used is in log-scale for better visualization purposes and for improved characterization of the near-source gradients.

C-PORT allows the user to view maps of pollutant concentrations, as well as difference maps between alternative scenarios. In addition to concentration maps, there is an option to download a shape file of the census block groups with the average concentration in each block group. Currently, a shape file is generated only for annual average model runs.

## 2.2. Software architecture

C-PORT is a web application consisting of a web interface, accessed via a web browser, a web service for retrieving and storing user data, a compute server for calculating dispersion results, and a database server. C-PORT can be run on any desktop/laptop computer, tablets, mobile devices, in any modern web browser and has been tested in Google Chrome, Firefox, and Safari. The most recent version of any browser is recommended. In order to use C-PORT, the browser must have JavaScript and cookies enabled. The recommended window size is at least 1200 by 800 pixels. The C-PORT web interface uses the Angular JavaScript framework with the Google Maps APIs. The web interface communicates with a web service built using the Python web framework Flask, running via the Gunicorn WSGI server behind the nginx web server. The web service makes use of several Python frameworks including SQLAlchemy-chempy, GeoAlchemy, pyproj (an interface to the PROJ4 library), Matplotlib, NumPy, SciPy, and PyShp. Dispersion model runs are submitted to a Linux compute cluster running RHEL 5.11 (Tikanga), to run a Fortran-based executable. Input source data, user data, and model run results are stored in a PostgreSQL database server, with the PostGIS extension to enable geographic support. See more info about the Linux Cluster at: <http://help.unc.edu/help/getting-started-on-killdevil/>. For more information on software/data availability, please contact The University of North Carolina at Chapel Hill, Institute for the Environment, 100 Europa Drive, Suite 490, Chapel Hill, NC 27517, T: (919) 966e2126, F: (919) 966e9920, Email: [cmas@unc.edu](mailto:cmas@unc.edu). C-PORT is currently available as a research grade screening tool in a password-protected status via CMAS (<https://www.cmascenter.org/c-tools/>). The user needs to register at the CMAS web site ([https://www.cmascenter.org/register/create\\_account.cfm](https://www.cmascenter.org/register/create_account.cfm)), and then use the CMAS account and password to access C-PORT. After logging in to the CMAS website, the user can access C-PORT for free and also get additional updates on C-PORT development, technical notes, and video tutorials.

### 2.3. Experimental testing of C-PORT

C-PORT has a map-based interface incorporating widely used Google Map (Fig. 5) as the underlying map engine. The web-based, interface is intended to provide nationwide coverage but currently includes data from 21 coastal ports (Baltimore, MD; Brunswick, GA; Charleston, SC; Gulfport, MS; Jacksonville, FL; Miami, FL; Mobile, AL; Morehead City, NC; New York/New Jersey; Palm Beach, FL; Panama City, FL; Pascagoula, MS; Pensacola, FL; Portland, OR; Port Canaveral, FL; Port Manatee, FL; Port of Virginia, VA; Savannah, GA; Seattle, WA; Tampa, FL; Wilmington, NC).

To test the functionality of the C-PORT, we selected Charleston, SC from the list of 21 coastal ports available in C-PORT (Fig. 6). After choosing a location, C-PORT loads all of the port-related data within the viewing window. Shipping channels are colored yellow, road links are colored pink, and rail lines are colored blue. Terminal polygons are colored green, while rail yard polygons are colored blue. Point sources are colored in orange. Squares represent the ship hoteling locations, while circles represent point sources (like a boiler) located within the terminal boundaries. For each source type, the user can modify existing data, as well as add or remove sources.

The “Perform Analysis” button opens a box that describes the model scenario. The user provides a scenario name, type of simulation (e.g. hourly diagnostic analysis, annual concentrations), selects the pollutant(s) of interest, selects meteorological conditions, and time period to be modeled (representative hourly or annual). In addition, the user can select individual or all source types to be included in the analysis. After submitting the model scenario for simulation, the user can click on the “View Results” box to check on the progress of the analysis, and when the run has completed, click on the “Eye Icon” and C-PORT will display the results of model simulations for selected scenario (Fig. 7). Similar analysis could be done for any of the 21 ports from the C-PORT menu.

C-PORT also allows the user to compare the model results with monitor data. The “Air Quality Monitors” button shows the location of Air Quality System (AQS) monitors that record ambient air pollution data. C-PORT displays the location of the AQS monitors and provides maximum and mean 1-h concentrations for recent years (2011-2015) for NO<sub>x</sub>, CO, SO<sub>2</sub>, and PM<sub>2.5</sub>. The AQS data summary, ingested from the EPA’s Air Data website (<https://www.epa.gov/outdoor-air-quality-data>) is a useful reference point for comparing C-PORT outputs. However, C-PORT does not consider background concentrations from other sources or regional background in the modeling domain. Therefore, C-PORT only provides estimates of the air quality impact of port operations at the local scale above regional background.

## 3. Results

We applied C-PORT to a portion of Charleston, SC to demonstrate its use. We used the results of a mobile monitoring study in Charleston to compare the relative contributions of various port terminals predicted by C-PORT to observed contributions during the monitoring study. These measurements represented the best data available for a comparison at this location and scale.



### 3.1. Case study area

The Port of Charleston, South Carolina, is currently one of the largest container ports in the United States, ranking 10th in terms of number of containers, and 40<sup>th</sup> by tons of cargo (*Statistical Abstract of the United States: 2012 (131st Edition). Tables 1086 and 1087.*). The South Carolina State Ports Authority (SCSPA) currently manages five facilities in the area: 1) the North Charleston terminal, handling primarily containers; 2) Wando Welch, the largest container terminal in the area; 3) Veterans terminal, designated as project cargo, including bulk materials; 4) Columbus Street terminal, also designated project cargo, including roll-on/roll-off; and 5) Union Pier terminal, used mostly for cruise ship operations.

Port trucks typically access I-26 and I-526 as the main transportation corridors (Fig. 6). They continue on these routes out of the city, or use them to deliver cargo to nearby multi-modal and rail yard facilities (other sources of port-related pollution) for subsequent distribution. Short-range drayage trucks typically deliver goods to these facilities, and are often the older and more polluting trucks of the fleet. The already congested I-26 is of particular concern due to expansion of the North Charleston terminal scheduled for completion in 2017, which is expected to increase traffic in the area by up to 7000 new truck trips per day, a 70% increase over the 10,000 truck trips that currently support container distribution.

The Charleston area has 14% of its population living below the federal poverty line and 25% in the low socio-economic category. Diverse neighborhoods surround the Charleston port areas, with relatively affluent communities also being located near ports; however, the low-income communities tend to be in closer proximity to multiple sources in their local areas. Residents in North Charleston, for example, are concerned about emissions from a nearby chemical plant, a cement factory, and wind-blown dust from coal piles. Low income communities tend to be concentrated near the roadways and rail yards as well, experiencing potential exposures from both onsite port operations as well as related traffic.

### 3.2. Mobile monitoring campaign

Mobile monitoring was conducted in Charleston, South Carolina from February 20, 2014 to March 13, 2014 (Steffens et al., 2017). The measurements were obtained using EPA's GMAP vehicle, an all-electric converted PT Cruiser designed for driving-mode high-resolution mobile sampling along roadways. It is outfitted with an array of on-board monitoring equipment to measure concentrations of various pollutants. Measured pollutants include ultrafine particles (EEPS, model 3090, TSI, Inc.), larger particles (APS, Model 3321, TSI, Inc.), NO<sub>2</sub> (CAPS, Aerodyne Research, Inc.), CO (quantum cascade laser, Aerodyne Research, Inc.), CO<sub>2</sub> (LI-COR), and black carbon (BC) (Aethalometer, Magee Scientific). Pollutant measurements are taken in real time at a 1 Hz sampling rate while vehicle latitude and longitude are recorded with on-board GPS (Crescent R100, Hemisphere GPS). Additionally, a portable stationary sampling station was used to capture 3D wind speed and direction (ultrasonic anemometer, RM Young).

Sampling occurred over 24 sessions. During each session, the GMAP vehicle was driven continuously along one of four predetermined routes. Sampling start times were selected to

be 4 a.m. for week one, 1:30 p.m. for week two, and 9 a.m. for week three. These times were chosen so as to not coincide with high-traffic times of day and to capture a variety of port operational hours. Normal port hours of operation are weekdays from 7 a.m. to 7 p.m. Each route requires approximately 30 min to complete. Vehicle battery allowed for approximately 3e4 h of continuous sampling, allowing for multiple laps per session. Three of the routes were selected for their proximity to different port terminals: Wando Welch Terminal, Columbus Street/Union Pier Terminals, and Veteran's Terminal (Fig. 6). The final route was near the Bennett Rail Yard. These routes are shown in Fig. 8. The routes are designed to be near the facility of interest and include at least one residential neighborhood.

Fig. 9 show the distribution of pollutant concentrations over all samples collected by mobile monitoring in four selected areas. These plots show concentration measurements under all meteorological and temporal conditions. As expected, the distributions of downwind concentrations are generally higher than upwind distributions, indicating the impact of the sources on nearby communities. The only exception is BC during stable conditions which could be due to a presence of a local source upwind of the Wando Welch terminal during this period of mobile measurements. The analysis also indicates a strong impact of atmospheric stability on levels of concentrations in the study areas.

### 3.3. Comparison with measurements

C-PORT provides estimates of air pollutant concentrations for a set of pre-selected representative weather categories (unstable, neutral and stable for winter and summer) based on hourly meteorological observations from the nearest National Weather Service (NWS) Station for 2011. Since the measurement campaign was conducted in 2014, direct model-to-monitor comparison would not be possible. Instead, we conducted a qualitative comparison to see if the model is capable of predicting spatial patterns of pollutant concentrations, and adequately responds to changes in meteorological conditions (e.g. slightly stable, neutral, and slightly convective conditions, and wind directions representing upwind/downwind conditions in residential communities near Wando Welch terminal). In this comparison, we focused on carbon monoxide, nitrogen oxides and carbon fraction of particulate matter as commonly used markers of traffic-related air pollution. While C-PORT provide estimates of primary CO, NO<sub>x</sub> and EC<sub>2.5</sub> (the portion of PM<sub>2.5</sub> consisting of elemental carbon), GMAP mobile measurements consisted of CO, nitrogen dioxide (NO<sub>2</sub>) and aethalometer-based BC. EC<sub>2.5</sub> is a model-based measure of a carbon fraction of particular matter while BC is a measurements-based measure of the carbon fraction, which is a commonly used marker of traffic-related air pollution, especially for diesel sources. Most NO<sub>x</sub> from combustion sources are emitted as NO, which is then readily converted to NO<sub>2</sub> in the ambient air; therefore, NO<sub>x</sub> and NO<sub>2</sub> will have similar concentrations for comparison purposes. C-PORT does not account for a portion of ambient NO<sub>2</sub> formed due to secondary production in the atmosphere. Also, C-PORT does not account for the background contribution, which is especially important for CO, yet near-source trends are comparable due to the impact of emission sources (see Fig. 9a).

Since a direct model-to-monitor comparison is not possible, we focused on a general comparison of upwind versus downwind concentrations for both C-PORT and GMAP

analysis, and subtracted the upwind portion of concentrations from the downwind to estimate a direct impact of emissions sources at Wando Welch terminal. We ran C-PORT for the Charleston domain for various meteorological conditions to estimate a range of air pollutant concentrations in areas where GMAP measurements were taken. Because GMAP monitoring campaign was from February 20, 2014, to March 13, 2014, we ran C-PORT for the winter weekday morning in slightly stable, neutral, and slightly convective conditions with a west-northwesterly winds to estimate pollutant concentrations in residential communities downwind of Wando Welch terminal. We also ran C-PORT for east-southwesterly winds to simulate the upwind conditions. The inspect mode in C-PORT allowed us to click anywhere on the map in the community downwind of Wando Welch terminal and get a predicted value for the concentration of the pollutants modeled.

The results of comparison between C-PORT and GMAP observations are shown in Table 1. As expected, C-PORT responds to changes in meteorological conditions, predicting higher concentrations during stable conditions and lower concentrations during unstable conditions. The model captures the impact of emission sources at Wando Welch terminal and predicts a range of concentrations at downwind receptors that overlaps with the 25–75 percentile range of observed concentrations from GMAP mobile measurements for all pollutants except CO during unstable conditions and BC during unstable and stable conditions. This discrepancy might be explained by a presence of some local sources or other confounding factors not captured by C-PORT.

## 4. Discussion and conclusions

C-PORT is a web-based, easy-to-use model that allows users to visualize and evaluate different planning scenarios to identify potential impacts, or weigh trade-offs among alternatives to facilitate decisions that protect community health and promotes sustainable solutions. C-PORT allows the user to modify input parameters, rerun the simulation, and compare the modified results with the unaltered (“base-case”) scenario. C-PORT also allows the user to add, delete, and modify emissions sources.

C-PORT offers the capability of producing scenario comparison maps. In the “View Results” menu, there is a tab for “Comparisons”. The user can run either “Absolute Difference” or “Relative Difference” comparison between two scenarios. Using the “Inspect Tool”, the user can develop a sense for how far the plume can impact the local community due to proposed changes in input conditions at the port.

### 4.1. Model advantages

The C-PORT modeling system incorporates a scientifically robust atmospheric dispersion algorithm, parameterized emission sources, and local meteorology to estimate air pollutant concentrations in the near-port communities. C-PORT uses a number of input parameters based on pre-loaded emissions and meteorological datasets with nationwide coverage but it also allows a user to upload and utilize local datasets that are likely of higher fidelity. An important feature of C-PORT is its ability to assess variations of a given scenario (i.e., its “*what-if*” capabilities), accurately describing relative differences between various inputs within the modeling domain, or relative changes in pollutant levels for a given port under

different conditions. For example, C-PORT can be used to: 1) identify potentially exposed populations to target resources and exposure-reduction efforts; 2) target outreach, education, and possible intervention for highly impacted community areas; 3) facilitate citizen science efforts to conduct air quality measurements by identifying areas for sensor-based measurements; 4) provide preliminary estimates of exposure to support subsequent detailed analyses; and, 5) examine potential concentration and spatial changes in air pollution given various emissions reductions strategies, such as alternative routes or clean fuels.

#### 4.2. Model limitations

It is important to note that C-PORT is not designed to be used for regulatory applications but instead should be considered a screening tool to specifically investigate air impacts associated with port operations, including major freight corridors for traffic, rail, and ships. C-PORT predicts long-term (annual average) and short-term (representative hourly) concentrations of multiple criteria and toxic air pollutants from port activities at very fine spatial scales in the near-source environment, with access through a web-based platform that requires minimal technical expertise to use. The model should not be used to calculate concentrations at specific locations for specific hours (e.g., using meteorological data from 1 p.m. on 20 January 2017). Instead, we recommend using C-PORT as a “diagnostic” tool to explore the impact of emission sources on a nearby community for a range of pre-selected meteorological conditions for shorter time periods, i.e. for a single hour which is considered to be representative of classic meteorological conditions that are conducive (or not) for dispersion of air pollutants. These meteorological conditions are based on hourly observations from the nearest NWS stations. The air dispersion calculations in C-TOOLS are based on scientifically robust formulations similar to those employed in regulatory models, but efficiencies are derived from specification of representative scenarios for the input data. Though functionally, C-TOOLS and regulatory models are similar in that they predict near source air quality, their application and intended purpose are distinctly different. Due to the specificity of a regulatory application, the use of such tools needs to follow strict protocols for data specification and model calculations. However, many community-scale applications require a quick initial assessment of air quality impacts to characterize the scope of the problem and guide more detailed analysis, and often do not require the rigor of a regulatory model application. C-TOOLS attempts to bridge this gap by combining air dispersion models with evolving web-based and visualization technologies to provide an easy-to-access and rapid screening tool for users to undertake such initial air quality impact assessments.

#### 4.3. Future development and availability

C-PORT is a part of the community-scale suite of screening tools called C-TOOLS (Community Air Quality Tools), developed by the US EPA to support community-level assessments of air quality scenarios. C-TOOLS are designed to provide an easily-accessible way to prioritize mitigation activities and evaluate the holistic trade-offs associated with many types of development (port, roadway, airport, energy facilities). The C-TOOLS suite includes several models: 1) C-LINE (already developed), 2) C-PORT (ongoing beta-testing), and 3) C-AIRPORT (currently under development).

C-LINE - the first member of the C-TOOLS suite - is a web-based modeling system whose front-end predicts concentrations of multiple air pollutants due to traffic emissions near roadways. C-LINE functionality has been expanded to model emissions from port-related activities (e.g. ships, trucks, cranes, etc.) to support a second, port-specific screening tool. The Community near-PORT modeling system (C-PORT) is capable of identifying potential locations of elevated air pollution concentrations near ports. As an easy to use alternative-scenario screening tool, C-PORT can be used by decision-makers, including port authorities, state and local governments, as well as local stakeholder groups who are concerned about environmental impacts and have an interest in identifying mitigation options. C-AIRPORT is intended to inform community decision-makers of local air quality impacts due to airport-related sources in their region of interest using an interactive, web-based modeling approach. Thus, all members of C-TOOLS modeling systems are intended to provide an accurate representation of near-source environmental conditions for a suite of important emission sources.

## Supplementary Material

Refer to Web version on PubMed Central for supplementary material.

## Acknowledgments

The U.S. Environmental Protection Agency, through its Office of Research and Development, partially funded and collaborated in the research described here under Contract EP-D-12-044 to the Institute for the Environment at the University of North Carolina at Chapel Hill (UNC-IE). We acknowledge Nathan Rice, Catherine Seppanen, Michelle Snyder, Alejandro Valencia, Jo Ellen Brandmeyer, Kevin Talgo, and Mohammad Omary of the UNC-IE for their contribution to C-PORT model development. We thank Jonathan Steffens and Sue Kimbrough of the US EPA for their contribution to the C-PORT evaluation in Charleston, SC. This paper has been subjected to Agency review and approved for publication. Approval does not signify that the contents reflect the views of the Agency nor does mention of trade names or commercial products constitute endorsement or recommendation for use. The views expressed in this article are those of the author(s) and do not necessarily represent the views or policies of the U.S. Environmental Protection Agency.

## Appendix A. Supplementary data

Supplementary data related to this article can be found at <http://dx.doi.org/10.1016/j.envsoft.2017.09.004>.

## References

- American Association of Port Authorities (AAPA). Ports' Value to the U.S. Economy. 2016. <http://www.aapa-ports.org/advocating/content.aspx?ItemNumber=21150> [Accessed July, 2016]
- Barzyk TM, Isakov V, Arunachalam S, Venkatram A, Cook R, Naess B. A near-road modeling system for community-scale assessments of mobile-source air toxics: the community line source (C-Line) modeling system. *Environ Model Softw*. 2015; 66:46–56.
- Carruthers DJ, Holroyd RJ, Hunt JCR, Weng WS, Robins AG, Apsley DD, Thompson DJ, Smith FB. UK-ADMS: a new approach to modelling dispersion in the earth's atmospheric boundary layer. *J Wind Eng Ind Aerod*. 1994; 52:139–153.
- Cimorelli AJ, Perry SG, Venkatram A, Weil JC, Paine RJ, Wilson RB, Lee RF, Peters WD, Brode RW. AERMOD: a dispersion model for industrial source applications. Part I: general model formulation and boundary layer characterization. *J Appl Meteorol*. 2005; 44:682–693.
- Cirillo MC, Polli AA. An inter comparison of semi empirical diffusion models under low wind speed, stable conditions. *Atmos Environ*. 1992; 26A:765–774.

- Chang SY, Vizuete W, Valencia A, Naess B, Isakov V, Palma T, Breen M, Arunachalam S. A modeling framework for characterizing near-road air pollutant concentration at community scales. *Sci Total Environ.* 2015; 538:905–921. [PubMed: 26363146]
- Olesen, HR., Berkowicz, RB., Løfstrøm, P. OML: Review of Model Formulation. National Environmental Research Institute; Denmark: 2007. p. 130NERI Technical Report No. 609 [www.dmu.dk/Pub/FR609.pdf](http://www.dmu.dk/Pub/FR609.pdf) [Accessed August, 2016]
- Rosenbaum A, Hartley S, Holder C. Analysis of diesel particulate matter health risk disparities in selected US harbor areas. *Am J Public Health.* 2011; 101:S217–S223. [PubMed: 21836118]
- Snyder MG, Venkatram A, Heist DK, Perry SG, Petersen WB, Isakov V. R-LINE: a line source dispersion model for near-surface releases. *Atmos Environ.* 2013; 77:748–756.
- Steffens, J., Kimbrough, S., Isakov, V., Deshmukh, P., Baldauf, R., Brown, R., Powell, A. Near-port air quality assessments utilizing a mobile monitoring approach. *Air Pollut Res.* 2017. (in press) Available online 17 April 2017 <http://dx.doi.org/10.1016/j.apr.2017.04.003>
- U.S. Environmental Protection Agency (EPA). Motor Vehicle Emissions Simulator (MOVES) User's Guide for MOVES 2010b. Office of Transportation and Air Quality; 2012 Jun. EPA-420-b-12e001b2012 <http://www.epa.gov/otaq/models/moves/documents/420b12001b.pdf> [Accessed July, 2016]
- U.S. Environmental Protection Agency (EPA). EJSCREEN User Guide. Office of Environmental Justice; 2016 Jun. 2016 [https://ejscreen.epa.gov/mapper/help/ejscreen\\_help.pdf](https://ejscreen.epa.gov/mapper/help/ejscreen_help.pdf) [Accessed August, 2016]
- Venkatram A, Strimatis D, Di Cristofaro D. A semi-empirical model to estimate vertical dispersion of elevated releases in the stable boundary layer. *Atmos Environ.* 1984; 18:823–928.
- Venkatram A, Horst TW. Approximating dispersion from a finite line source. *Atmos Environ.* 2006; 40:2401–2408.
- Weil, JC. Plume rise. In: Venkatram, A., Wyngaard, JC., editors. *Lectures on Air Pollution Modeling.* American Meteorological Society; Boston, MA: 1988. p. 119-166.
- Zartarian VG, Schultz BD, Barzyk TM, Smuts M, Hammond DM, Medina-Vera M, Geller AM. The EPA's community-focused exposure and risk screening tool (C-FERST) and its potential use for environmental justice efforts. *Am J Public Health.* 2011; 101(S1):S286–S294. [PubMed: 22021316]



**Fig. 1.**  
Emission sources at a port terminal represented by point sources.



**Fig. 2.**  
Emissions from roadways and rail represented by line sources.



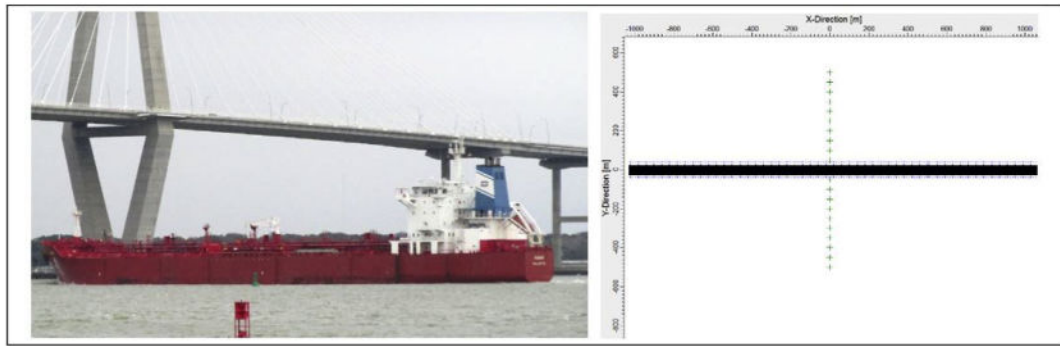


**Fig. 3.**  
Emission from ships in transit represented by buoyant line sources.



**Fig. 4.**  
Emission sources at a port terminal represented by an area source.

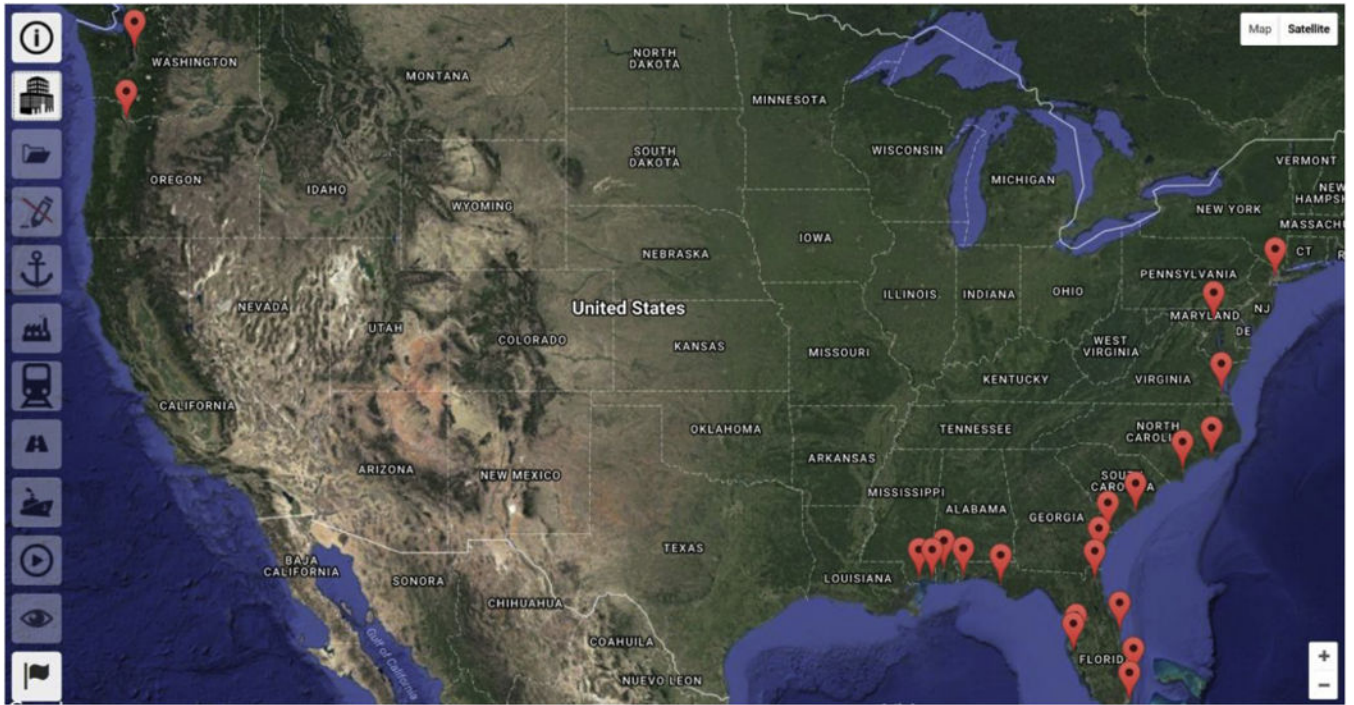


**Fig. 5.**  
C-PORT interface showing locations of available coastal sea ports.

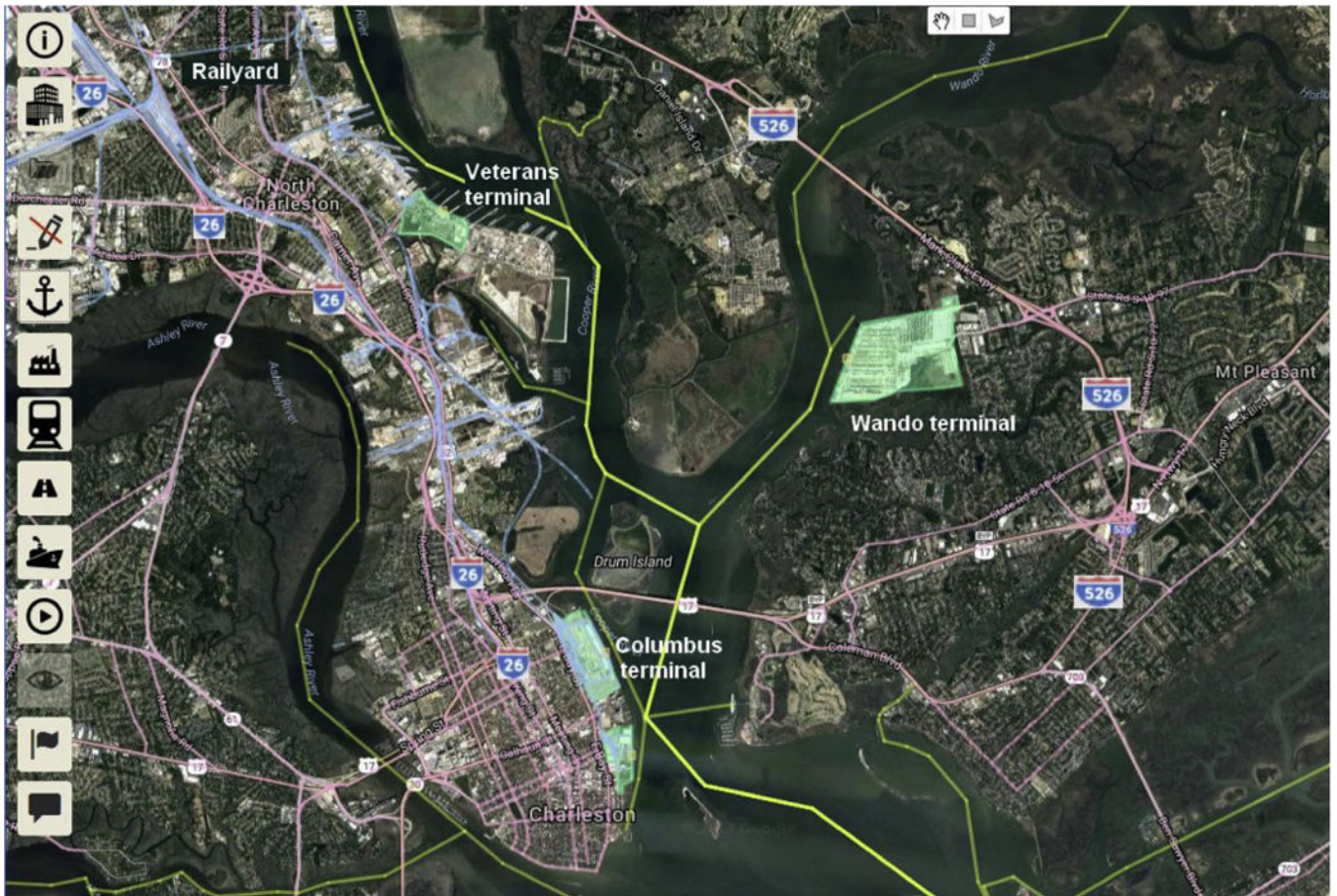


**Fig. 6.** Geographic domain in Charleston, SC showing locations of port terminals, roadways, railyards, shipping lanes, and main transportation corridors I-26 and I-526.



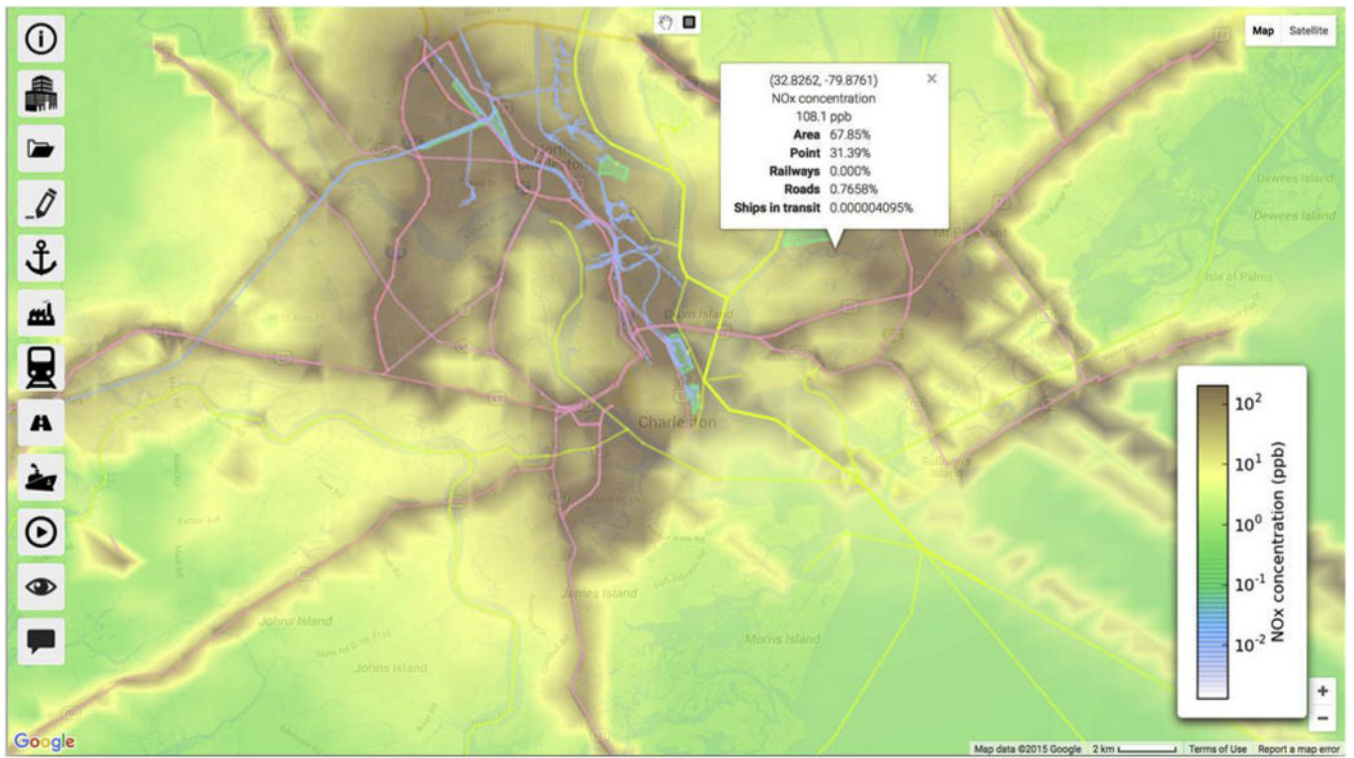


**Fig. 7.**  
Example of C-PORT application in Charleston, SC, showing NOx concentrations.

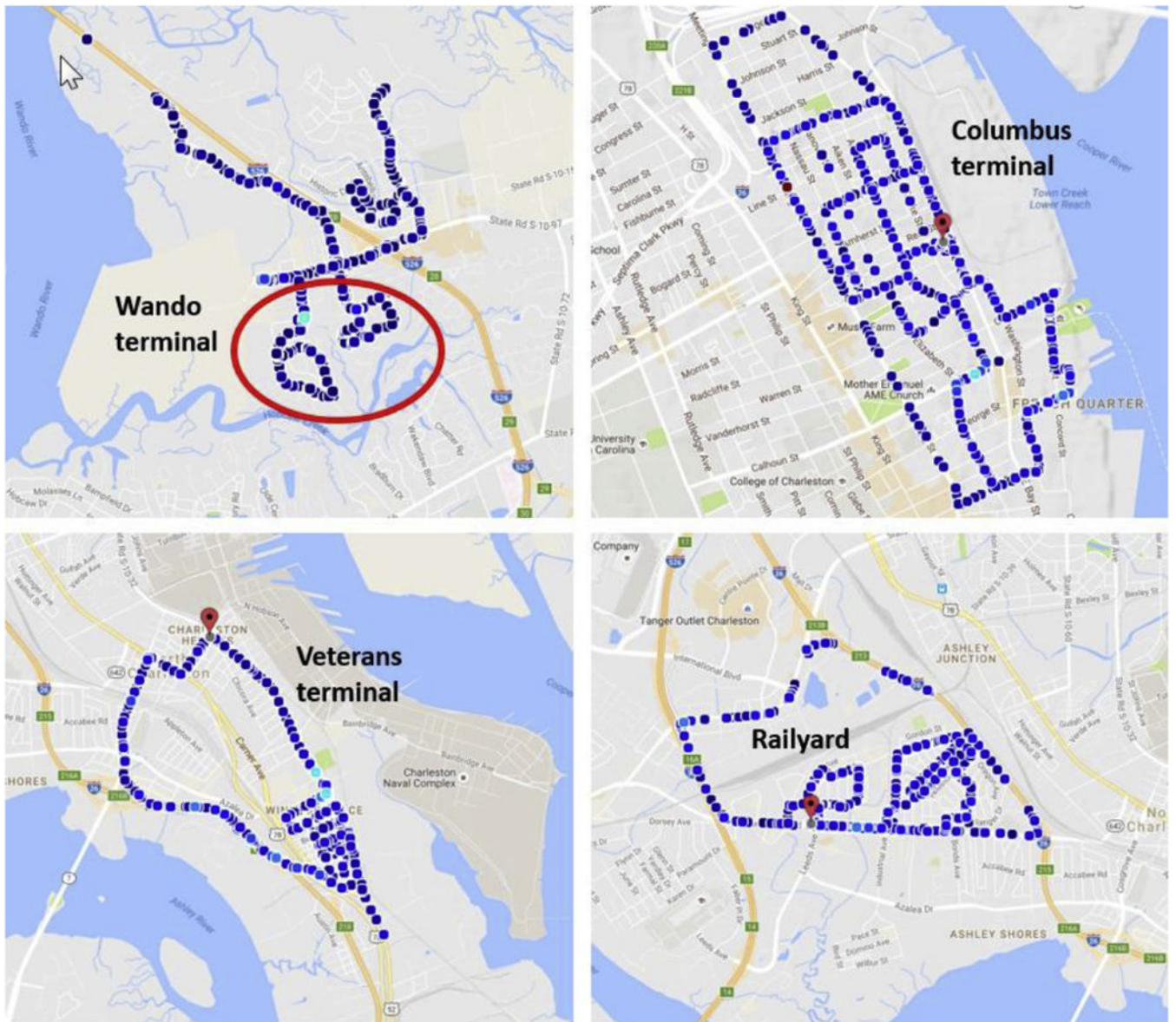
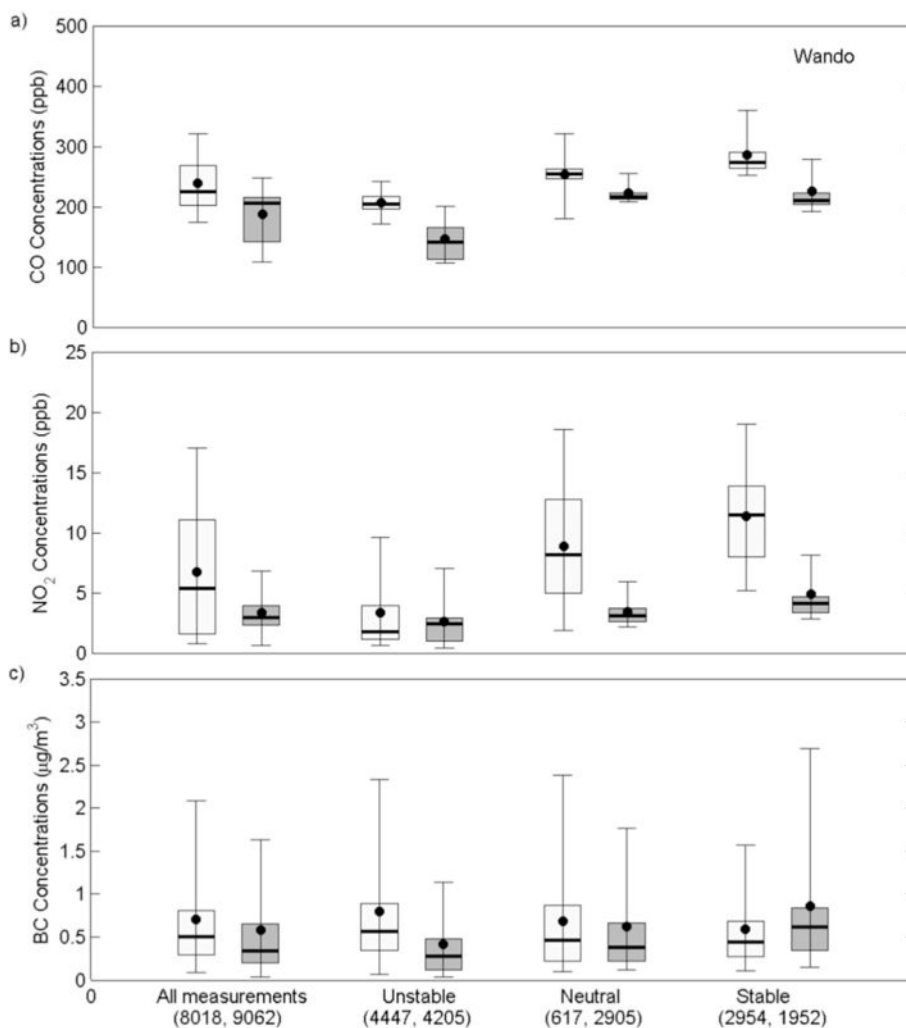


Fig. 8. GMAP driving routes in four monitoring sections around port terminals.



**Fig. 9.** Distributions of observed CO (a), NO<sub>2</sub> (b), and BC (c) concentrations from mobile monitoring downwind (light gray) and upwind (dark gray) of Wando Welch terminal for various stability conditions during the entire study. Each distribution is based on  $n$  observations (shown in parentheses below labels). The middle line represents the median, the box the 25th and 75th percentiles, and the whiskers the 5th and 95th percentiles. The data point represents the mean value of the distribution.

**Table 1**

Comparison between estimates of impact of emissions from the Wando Welch terminal on downwind concentrations based on GMAP measurements and estimates based on C-PORT model predictions.

<b>Carbon monoxide</b>		
Atmospheric stability	25–75 percentile range of difference between downwind and upwind CO (ppb) concentrations from GMAP measurements	Range of differences between downwind and upwind CO (ppb) concentrations from C-PORT model predictions
unstable	50.5–84.3	0.3–11
neutral	34.4–39.6	0.5–42
stable	59.9–67.4	2–84
<b>Nitrogen oxides</b>		
Atmospheric stability	25–75 percentile range of difference between downwind and upwind NO <sub>2</sub> (ppb) concentrations from GMAP measurements	Range of differences between downwind and upwind NO <sub>x</sub> (ppb) concentrations from C-PORT model predictions
unstable	0.09–1.0	0.4–1.9
neutral	2.3–9.1	0–2.6
stable	4.6–9.2	0–6.1
<b>Carbon fraction of particulate matter</b>		
Atmospheric stability	25–75 percentile range of difference between downwind and upwind BC (µg/m <sup>3</sup> ) concentrations from GMAP measurements	Range of differences between downwind and upwind EC25 (µg/m <sup>3</sup> ) concentrations from C-PORT model predictions
unstable	0.22–0.41	0–0.1
neutral	0.01–0.20	0–0.3
stable	–0.07–0.15	0–0.7